ARTICLES

Bounded cascade models as nonstationary multifractals

A. Marshak,* A. Davis,† R. Cahalan, and W. Wiscombe
NASA Goddard Space Flight Center, Climate and Radiation Branch, Greenbelt, Maryland 20771
(Received 1 July 1993)

We investigate a class of bounded random-cascade models which are multiplicative by construction yet additive with respect to some but not all of their properties. We assume the multiplicative weights go to unity as the cascade proceeds; then the resulting field has upper and lower bounds. Two largely complementary multifractal statistical methods of analysis are used, singular measures and structure functions yielding, respectively, the exponent hierarchies D_q and H_q. We study in more detail a specific subclass of one-dimensional models with weights $1\pm(1-2p)r_{n-1}^{H}$ at relative scale $r_n=2^{-n}$ after n cascade steps. The parameter $H>0$ regulates the degree of nonstationarity; at $H=0$, stationarity prevails and singular "p-model" cascades [Meneveau and Sreenivasan, Phys. Rev. Lett. **59**, 1424 (1987)] are retrieved. Our model has at once large-scale stationarity and small scale nonstationarity with stationary increments. Due to the boundedness, the D_q all converge to unity with increasing n; the rate of convergence is estimated and the results are discussed in terms of "residual" multifractality (a spurious singularity spectrum due to finite-size effects). The structure-function exponents are more interesting: $H_q=\min\{H,1/q\}$ in the limit $n\to\infty$. We further focus on the cases $q=1$, related to the fractal structure of the graph, $q=2$, related to the energy spectrum, and $q=1/H$, the critical order beyond which our multiplicative (and multiscaling) bounded cascade model can be statistically distinguished from fractional Brownian motion, the corresponding additive (and monoscaling) model. This bifurcation in statistical behavior can be interpreted as a first-order phase transition traceable to the boundedness, itself inherited from the large-scale stationarity. Some geophysical applications are briefly discussed.

PACS number(s): 02.50.−r, 05.40.+j

I. INTRODUCTION

A. Turbulent cascades as stationary scale-invariant processes

Multiplicative cascade models have enjoyed a growing popularity over the past decade, ever since the introduction of multifractal formalism [1–4]. Many different data-analysis techniques based on multifractal concepts have been developed and the range of problems to which they (as well as cascade models) have been successfully applied spans laboratory, geophysical and astrophysical systems. Multifractal formalism has become a virtually indispensable tool in computational physics where applications include percolating systems, growth phenomena (such as diffusion-limited aggregation) and deterministic chaos. The common feature in all of the above situations is the strongly nonlinear dynamics and the large range of spatiotemporal scales. It is no accident that the earliest and still one of the main sources of motivation for introducing new cascade models is the characterization of inhomogeneity ("intermittency") in turbulence at the dissipation scale and its effect ("corrections") on the inertial range quantities and associated exponents. This fruitful interaction was initiated prior to the development of the general formalism, in the pioneering studies following Kolmogorov's "refined" similarity hypothesis [5–9], was actively pursued while the multifractal formalism was being elaborated [10–13], and continues to stimulate new ideas [14,15].

An important property of all currently available turbulent cascade models is "stationarity," an expression we borrow from time-series analysis meaning "(statistical) invariance under translation." We will extend this definition to the spatial domain as well and will do without the mathematically correct but potentially confusing expression of "(statistical) homogeneity." Stationarity is generally viewed as desirable property *a priori,* on theoretical grounds. Let $\varphi(x)$, $0\le x\le L$, designate a generic random process with a finite one-dimensional support and let $\langle\ \rangle$ denote ensemble or φ averaging. The common assumption that $\langle\varphi(x)\rangle\equiv 0$ has no bearing on stationarity. Brownian motion is the classic case of nonstationarity; if starting at $\varphi(0)=0$, it will verify this assumption but also yields $\langle\varphi(x)^2\rangle\sim x$. Switching from one- to two-point statistics, an autocorrelation function

$$G(r;x)=\langle\varphi(x)\varphi(x+r)\rangle\ ,\quad 0\le x\le L-r\quad(0\le r\le L)\ , \tag{1}$$

independent of x, $G(r;x)\equiv G(r)$, is already a good indication of stationarity. If $\varphi(x)$ is furthermore scale invariant over all possible scales, $0<r\le L$, then

$$G(r)\sim(r/L)^{-\mu}\ ,\quad 0<\mu<1\ . \tag{2}$$

*Also at Science Systems and Applications, Inc. (SSAI), 5900 Princess Garden Parkway, Lanham, MD 20706.

†Also at Universities Space Research Association (USRA), NASA-GSFC (Code 610.3), Greenbelt, MD 20771.

1063-651X/94/49(1)/55(15)/$06.00

The Wiener-Khintchine theorem states that the energy spectrum $E(k), 1/L \leq k < \infty$, is in Fourier duality with $G(r)$. In the scaling case (2), we have

$$E(k) \sim (kL)^{-\beta}, \quad 0 < \beta = 1 - \mu < 1 . \tag{3}$$

Notice that the exponents μ and β have the same natural range: correlation will generally decrease with increasing separation ($\mu > 0$, $\beta < 1$) but a too rapid decay ($\mu \geq 1$) is basically equivalent to a δ correlation, $\beta \to 0$ ($\mu \to 1$) leads to $G(r) \to \delta(r)$ (i.e., μ becomes irrelevant).

From another vantage point, stationarity is an undesirable constraint since many natural signals, in fact, exhibit both scaling and nonstationary behaviors, i.e., they empirically yield $\beta > 1$. Prime examples come again from turbulence: velocity [16] and passive scalar [17,18] fluctuations have $\beta = \frac{5}{3}$ and many other geophysical signals are also in this category. To mention only those of immediate interest to the authors, we have (cloud) liquid water content [19–21] and the Earth's radiation fields [22]. A prototypical scale-invariant nonstationary process is provided by any coordinate of a particle in Brownian motion and the focus has been mainly on its geometrical or "self-affine" properties. Further examples of statistical self-affinity are Mandelbrot's [23] fractional Brownian motions (FBM's). However, these simple scaling models lack intermittency, even in their (stationary) gradient fields; "activity" is diluted in all of space, not concentrated onto sparse fractal subsets as in cascade models. Also these models are "too nonstationary," in the following sense: given an infinite domain of definition, they can wander off to $\pm\infty$ whereas many fields related to natural phenomena are physically bounded. It is possible to have the best of both worlds of scaling behavior, nonstationarity and intermittency? Not straightforwardly, to say the least, since the former attribute calls for additive models (hence simple scaling) while the latter calls for multiplicative models (hence multiple scaling).

B. From intermittent random measures and stationarity to random multiaffine functions and nonstationarity

An increasing number of researchers are looking at this problem. Parisi and Frisch's original description of multifractality [3], based on local Hölderian properties, is a rich but somewhat abstract conceptualization. In particular, they do not describe in any concrete way how to build a multifractal. Schertzer and Lovejoy [11] suggested a simple power-law filtering (fractional integration) of singular cascade models as a means to stochastically simulate fields reminiscent of passive scalars in turbulence. In the same spirit but instead of smoothing the completed cascade in Fourier space, one can simply act on the multiplicative weights during the cascade in physical space [24]; this is the approach we explore in more detail in the following. The midpoint displacement technique for building FBM's were generalized in Refs. [25–27] to obtain random or deterministic functions with multiple Hölderian singularities. The same goal was achieved by combining (fractional or ordinary) integration with signed measures obtained by recursive cascade-like procedures in Refs. [28–30].

Clearly, we are dealing with a vast and important new class of stochastic models that have been accurately described as "multiaffine" [26,27]. In contrast with (standard, unbounded) cascade processes which only exist, mathematically speaking, in the sense of measures (i.e., via integrals), multiaffine processes are simply random functions, as are their "monoaffine" counterparts (namely, FBM's). Accordingly, different statistical tools are needed to characterize the two above types of multifractals. On the one hand, standard singularity analysis techniques (which we will refer to generically as "singular measures") apply to multiplicative cascades which are stationary. On the other hand, structure functions apply to multiaffine processes which are necessarily nonstationary. In fact, we will argue that the structure function exponents give us a way of quantifying and qualifying "nonstationarity," a presently rather fuzzy notion, in much the same way as standard singularity analysis makes precise the concept of "intermittency," a previously fuzzy attribute of variability.

C. Overview and scope of this paper

In the upcoming section, we survey the theory of multiplicative cascades and introduce the general idea (and some specific ways) of smoothing the singularities as they develop, by reducing at each cascade step the dispersion of the multiplicative weights. We stress the fact that such models have both stationary and nonstationary features, scaling regimes in particular. In Sec. III, bounded models are studied from the standpoint of singular measures and we find that the generalized dimensions converge towards triviality ($D_q \equiv 1$) as the cascade develops. In other words, we find a dramatic but not total collapse of the singularity spectrum since, at finite resolution, there is a finite "residual" D_q spectrum of interest in its own right. In particular, the finding of such spurious intermittency exponents rises important questions about how to interpret the results of singularity analysis when applied to intrinsically bounded atmospheric fields, e.g., reflected solar flux or liquid water density in clouds.

In Sec. IV, we turn to structure functions and find the associated exponents $\zeta(q)$ to exhibit definite multiscaling in the bounded case. As might be expected from their stationarity, we find trivial structure functions [$\zeta(q) \equiv 0$] for standard cascades. Cases of special interest are discussed in more detail: at $q = 1$ we find the model to be stochastically continuous and at $q = 2$ we find β values in excess of unity, as required (except in the singular limit of the model). We systematically compare the new models with FBM's, the latter being nonstationary on all scales whereas the former are only asymptotically (small-scale) nonstationary. This apparently subtle difference induces a multifractal phase transition of the first kind: the first derivative of $\zeta(q)$ is discontinuous at a critical q related to the new (smoothing) parameter. In Sec. V, we summarize and discuss our findings using, in particular, the "$q = 1$ multifractal plane" which is a simple device for pinpointing the degrees of intermittency and of nonstationarity in any system or model.

Throughout the following, we will use exclusively moment-based statistical approaches. In Ref. [31] we re-

cast and discuss our main results in terms of local Hölderian singularity analysis in the manner of Parisi and Frisch [3].

II. MULTIPLICATIVE CASCADE MODELS

A. Turbulent cascades in general, log-binomial p models in particular

Consider a homogeneous distribution of some substance on the unit interval. Let $\phi_n(x_m)$ be the mth part of the substance distribution after the nth step. First ($n=1$) we divide the unit interval into λ_0 equal parts of length $1/\lambda_0$ ("subeddies") where λ_0 is an integer >1 and then the non-negative random weights $W_{1j}, j=1,\ldots,\lambda_0$, are applied [see Fig. 1(a) for an example with $\lambda_0=3$]. In the next step ($n=2$) each subinterval is further divided into λ_0 equal parts with corresponding weights $W_{2j}, j=1,\ldots,\lambda_0$ [Fig. 1(b)] and so on [see Figs. 1(c) and 1(d) where we use the more traditional [32] notation "ϵ" instead of "ϕ"]. On the nth step the distribution of the original substance is

$$\phi_n(x_{\lambda_0 m-j+1})=\phi_{n-1}(x_m)W_{nj}\ , \qquad j=1,\ldots,\lambda_0\ ,\quad m=1,\ldots,\Lambda_{n-1}\ , \tag{4}$$

starting with $\phi_0(x_1)=1$ and where

$$\Lambda_n=\lambda_0^n\ ,\quad n=1,2,\ldots, \tag{5}$$

is the number of cells in the lattice and

$$r_n=1/\Lambda_n \tag{6}$$

is the variable grid constant, in other words, the vanishing inner or homogeneity scale.

It follows from (4) that

$$\phi_n(x_m)=\prod_{i=1}^{n} W_{ij}\ ,\quad m=1,\ldots,\Lambda_n\ ,\quad n=1,2,\ldots, \tag{7}$$

where j randomly takes one of its λ_0 values as the cascade proceeds. When n is large enough the above processes can be highly intermittent and are generally referred to as "multifractals," emphasizing the multiplicative modulation and the sparseness of the sets where the substance is ultimately concentrated. This, however, calls for W_{ij}'s that are identically distributed with respect to $i=1,2,\ldots,n$ (or at least have comparable dispersions).

If the W_{ij} are log-normally distributed random numbers (exponentials of normal deviates with mean M and standard deviation σ), independently of $i=1,2,\ldots,n$ (and $j=1,\ldots,\lambda_0$), we obtain the cascade model first proposed in [5,6] as an attempt to account for intermittency in fully developed three-dimensional (3D) turbulence. To keep the model conservative on average ($\langle W\rangle=1$) one requires $M=-\sigma^2/2$. The outcome for $\lambda_0=3$ and $\sigma=0.5$ is illustrated in Figs. 1(a)–1(d) for $n=1$, 2, 4, and 6. Notice how, on the one hand, the number of cells is multiplied by λ_0 at each step and how, on the other hand, the peaks grow in strength with no bounds in view; the vertical scale (in the inset) gives a rough idea of this growth.

For $\lambda_0=2$ we obtain another turbulent cascade model known as a "p model" [13] by letting W_{i1} be either $2p$ or $2(1-p)$, $0\le p\le 1/2$, with equal probability, and $W_{i2}=2-W_{i1}$ (still independently of $i=1,2,\ldots,n$). This model is constrained to be microcanonically [8] conserved (i.e., on a per eddy basis), less restrictive canonical versions (the weights are independent from one subeddy to the next, as in the log-normal model) have also been proposed [10]. The p model can also be related to the dynamical systems concept of a "two-scale Cantor set" [4].

It follows from (7) that

$$\log_{\Lambda_n}\phi_n(x_m)=\frac{1}{n}\sum_{i=1}^{n}\log_{\lambda_0}W_{ij}\ . \tag{8}$$

If the weights can only take one of two values, then after n cascade steps there are $n+1$ different levels equally

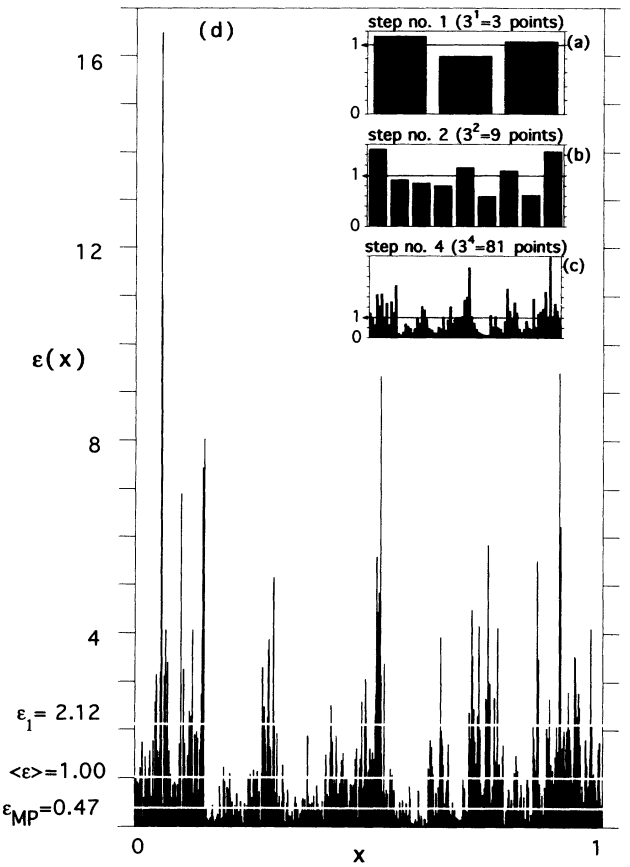

FIG. 1. Development of a canonical log-normal cascade model $\epsilon(x)$, $0\le x\le 1$, with dividing ratio $\lambda_0=3$ and standard deviation $\sigma_{\ln W}=0.5$, recalling that we take mean $M_{\ln W}=-\sigma^2_{\ln W}/2$ to obtain $\langle W\rangle=\langle\epsilon\rangle=1$. Cascade steps $n=1$, 2, and 4 are found in the inset, illustrating the unbounded growth of singularities of all orders (the arrows indicate the unit average). The sixth step is illustrated in more detail, with average $\langle\epsilon\rangle$ and most probable values highlighted ϵ_{MP} as well as the value ϵ_1 that contributes most to the (unit) mean $\langle\epsilon\rangle$. The "information" codimension $C_1\approx 0.11$ can be visualized with the help of the level- or exceedence-set associated with ϵ_1 (fractal dimension $D_1=1-C_1$).

spaced between two extremes on a log scale as in (8); moreover, these levels (or "orders of singularity") are binomially distributed. We will therefore refer to the p model as a "log-binomial" model, thus emphasizing the essential difference with its log-normal counterpart, the statistical properties of any multiplicative cascade model being completely determined by the choice of weights, equivalently, their logs (the "generators" [11]).

Cascades come with all degrees of intermittency between two extremes. If both multiplicative weights are always equal ($p=\frac{1}{2}$ in the above) the field remains flat and we can take this case of degenerate weights as representative of "weak" variability, fluctuations around some nonvanishing mean value of small amplitude relative to this mean. At the other extreme on the intermittent variability scale we find the case where the smaller of the two possible weights is null ($p=0$ in the above). Instead of being randomly "strengthened" or "weakened," the subeddies are made "dead" or maintained "alive." Every time a $-\infty$ is contributed to the sum (8), no number of subsequent positive contributions will balance it and all surviving eddies will be equally strong. One could legitimately talk about "log-monomial" models but these are generally referred to as "β models" [9] or "monofractals" [11]. In this case, the (microcanonical) log-binomial model reduces to a single Dirac δ function centered at random in the unit interval, an extreme case of intermittency by any standard.

There are degrees of intermittency and kinds of intermittency. The problem of intermittency in turbulence has motivated singular cascade models with many different flavors: log-normal [5,6], log-binomial (i.e., α models [10] or p models [13]), log-Levy [11], log-monomial (β models [9], also [7,8]), and even log-degenerate (for constant fields). It all depends on the distribution of the multiplicative weights. The model to be introduced shortly is a simple variant on the p model that shifts the focus entirely from the issue of homogeneity vs intermittent variability (and what kind) to that of stationarity vs nonstationarity.

It can be shown [32] that all multiplicative cascade processes (with weights W independent of the cascade step) have scaling autocorrelation functions with exponents $\mu=\log_{\lambda_0}\langle W^2\rangle$ and energy spectra with exponents $\beta=1-\mu<1$. For instance, the spectral exponent of the log-binomial model is $\beta=1-\log_2[1+(1-2p)^2]$ and the log-normal one has $\beta=1-\sigma^2/\ln\lambda_0$. This constraint of stationarity—and the related one on β—considerably limits the direct applicability of cascade models since natural signals or fields very often have $\beta>1$, as mentioned in the Introduction. Scaling models with nonstationary small-scale behavior ($\beta>1$) are typically additive in nature (e.g., FBM's). In the following, we will describe a way of constructing such random fields without leaving the general framework of multiplicative cascades. This is appealing because, as is widely believed to occur in turbulent flows, cascade processes will arguably occur whenever nonlinearity dominates the dynamics of the system. We will then investigate the multifractal properties of the new model.

B. Bounded cascade models

Consider microcanonical cascade models with $\lambda_0=2$, i.e., where

$$W_{ij}=1\pm f_i \quad (0\le f_i\le 1, j=1,2)\ . \tag{9a}$$

If

$$f_i\to 0\ ,\quad i\to\infty\ , \tag{9b}$$

then these models,

$$\phi_n(x_m)=\prod_{i=1}^{n}(1\pm f_i)\ ,\quad m=1,\ldots,\Lambda_n\ , \tag{10}$$

lose their log-binomial character and accept upper and lower bounds ($\phi_\pm$):

$$0<\phi_-\le\phi(x)=\lim_{n\to 0}\phi_n(x)\le\phi_+<\infty\ ,\quad 0\le x\le 1\ . \tag{11}$$

The following parametrization has been suggested in somewhat different notations [24]

$$f_i=\frac{(1-2p)2^H}{2^{Hi}}\ ,\quad 0\le p\le\tfrac{1}{2}\ ,\quad 0\le H\le\infty\ . \tag{12}$$

Explicitly, we have $f_1=1-2p$, $f_i=f_{i-1}/2^H$, $i=2,3,\ldots,n$. Many other models with vanishing f_i are conceivable, e.g., the more general three-parameter version of the above $f_i=(1-2p)2^H i^s/2^{Hi}$ with $s\ge 0$.

At $H=0$ the bounded model reverts to a standard (unbounded, stationary) log-binomial one with its special extreme cases described previously. The parameter H clearly produces a radical smoothing that converts cascades of the usual singular kind into more tame bounded processes. The composite Fig. 2 dramatically illustrates this point, using a sequence of "zooms" onto a cascade model with $H=\frac{1}{3}$ and $p=0.35$ ($\phi_-=0.289\cdots$, $\phi_+=2.96\cdots$). Each of the graphs contains $2^9=512$ points. Figure 2(a) is a $n=9$ level bounded cascade. It is then divided into 16 parts and one of them is horizontally rescaled and details are added using four more cascade steps locally [Fig. 2(b)]; this leads to $\frac{1}{16}$th of the same cascade at $n=13$ levels. This procedure is repeated twice more [Figs. 2(c) and 2(d)] up to $n=21$. One sees that the increase of n essentially "regularizes" the field. In mathematical terminology, the resulting process is "stochastically continuous." Figures 2(b')–2(d') are vertically rescaled versions of Figs. 2(b)–2(d). Clearly, these all look similar and this illustrates a basic scaling property of $\phi(x)$: its graph is statistically self-affine (see Sec. IV for further details). The "smoothing" effect of H can also be demonstrated by considering an extreme case. If we take the limit $H\to\infty$ we are left with one single jump at $x=0.5$, all other cascade steps are ineffective. This special case is therefore mapped to a Heaviside step, randomly up or down. This is a prime example of nonstationarity and almost everywhere differentiability over and above stochastic continuity (which is not inhibited by a single discontinuity in every realization).

Strictly speaking, the above models are not scale invariant over the full range of available scales. One can

define a characteristic scale r^* dependent on H such that r^{*H} equals $\frac{1}{2}$. Solving $r^{*H}=\frac{1}{2}$ for a (not necessarily integer valued) characteristic cascade "step" we find

$$n^* \approx 1/H \ . \tag{13}$$

Up to this point, the ϕ_n values change considerably as n is incremented; from then on, the f_i can be considered $\ll 1$ to first order and the ϕ_n values change much less. Qualitatively speaking, the model behaves "multiplicatively" for the largest scales ($r \gtrsim r^*$) implying a degree of stationarity and discontinuity whereas, for the smallest scales ($r \ll r^*$), the model's behavior is dominated by the smoothing. As we will see, continuity and "additive" features arise and stationarity can be found only in the increments. We note however that, for finite values of H (a typical value of interest is $\frac{1}{3}$, n^* is $O(1)$ and for a finite $n \gg n^*$ there exists a large scaling regime where the exponents discussed in the following are defined either numerically or analytically.

III. SINGULARITY ANALYSIS

A. Brief description

Define the generic stochastic process [43]

$$\varphi(x) \geq 0 \ , \quad 0 \leq x \leq L \ . \tag{14}$$

For simplicity, we have assumed that the dimension of the "support" (the L-sized interval where x takes its values) is one. Define also the open segment, $B_r=(-r/2,+r/2)$, $0<r\leq L$, and its indicator function

$$I_{B_r}(x)=\begin{cases}1, & x\in B_r \ , \quad 0<r\leq L \\ 0 \ , & x\notin B_r \ , \quad 0<r\leq L \ .\end{cases}$$

Now, keeping r constant, consider the following convolution product of the random process $\varphi(x)$ and $I_{B_r}(x)$ which we denote by "$\Sigma\varphi$." Then

$$\begin{aligned}\Sigma\varphi(r;x)&=[\varphi \circ I_{B_r}](x) \\ &=\int_0^L \varphi(x')I_{B_r}(x-x')dx' \\ &=\int_{x-r/2}^{x+r/2}\varphi(x')dx' \ , \quad r/2\leq x\leq L-r/2 \ .\end{aligned} \tag{15}$$

Since we will be seeking power-law behavior, it is best to normalize the random measures in (15), the natural choice being

$$p_r(x)=\frac{\Sigma\varphi(r;x)}{\langle \Sigma\varphi(L;L/2)\rangle}\geq 0 \ , \tag{16}$$

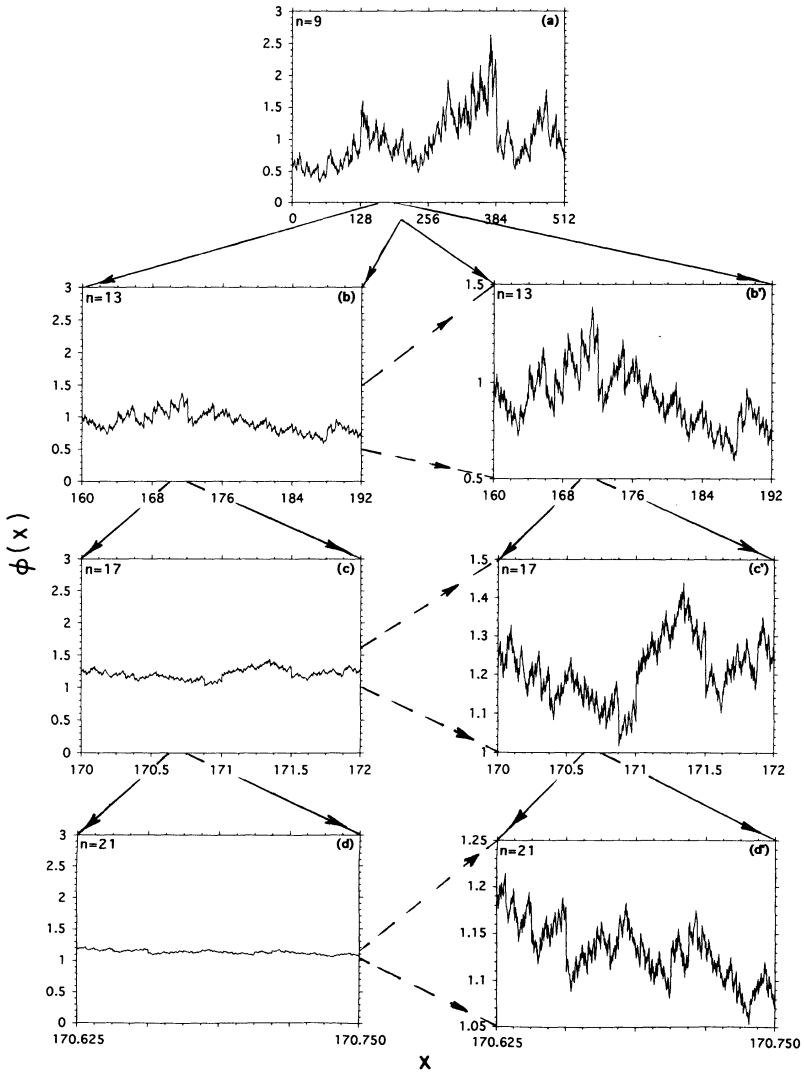

FIG. 2. Visualization of the continuity and self-affine properties of a bounded cascade model $\phi(x)$, $0\leq x\leq 2^8$, with $h=\frac{1}{3}$ ($\beta=\frac{5}{3}$) and $p=0.35$. (a) The complete field for $n=9$ with bounds $\phi_-=0.289\cdots$ and $\phi_+=2.96\cdots$ and unit average; (b) $n=13$, horizontal rescaling of (a); (c) $n=17$, horizontal rescaling of (b); (d) $n=21$, horizontal rescaling of (c). (b') $n=13$, vertical rescaling of (b); (c') $n=17$, vertical rescaling of (c); (d') $n=21$, vertical rescaling of (d). Notice the similarity of panels a,b',c',d' ($D_{g(\varphi)}=\frac{5}{3}$) and the vanishing increments (stochastic continuity) along the sequence a,b,c,d.

which is not to be confused with the parameter p in the cascade model (12).

We assume here that the stochastic process $\varphi(x)$ is stationary; for our present purposes, this means that statistical moments are independent of position, i.e., $\langle p_r(x)^q\rangle = \langle p_r^q\rangle$ for any real q. Of course in practice, one will tend to (make "ergodicity" assumptions and) substitute spatial or x averaging for its ensemble or φ counterpart. This can be for reasons of computational cost (models) or because very few realizations are available, possibly only one (data). At any rate, the case $q=1$ is easily dealt with; using (15) and (16), we find

$$\langle p_r\rangle = \frac{r}{L} , \tag{17a}$$

assuming from now on that $p_r(x)\neq 0$ almost surely. For $q\neq 1$, we get

$$\langle p_r^q\rangle \sim \left[\frac{r}{L}\right]^{1+\tau(q)} , \quad r \ll L \tag{17b}$$

with $\tau(1)=0$ due to (17a) and $\tau(0)=-1$ due to normalization. Actually, we consider only the moments of order q for which $\langle p_r^q\rangle < \infty$. The conditions for divergence of high-order moments are briefly discussed in Appendix A but in the following we will not be concerned with this complication since microcanonical conservation guarantees convergence, even in the limit $q\to\infty$ [33].

If the random field $\varphi(x)$ is quasihomogeneous (say, narrowly bounded above and below, everywhere and on all scales), then $\langle p_r^q\rangle \approx \langle p_r\rangle^q = (r/L)^q$ (for all r and q) and (17b) yields $1+\tau(q)=q$. In contrast, if $\tau(q)\neq q-1$ for all $q\neq 0,1$, then it is concave [$\tau''(q)<0$] and we are dealing with very skewed inhomogeneous fields: $\langle p_r^q\rangle$ will generally be very different from $\langle p_r\rangle^q$ since even a small difference in the exponents causes a large difference in moments due to the smallness of r/L. On the one hand, this leads to the idea of generalized or Renyi dimensions [1,2]

$$D_q = \frac{\tau(q)}{q-1} \tag{18}$$

which is $\equiv 1$ in weakly variable situations and nonincreasing generally speaking. On the other hand, the Legendre transform of $\tau(q)$ yields the well-known singularity spectrum $f(\alpha)$, conveying upon it a multifractal meaning [4]: the leading contributions to $\langle p_r^q\rangle$ come from ever sparser (more fractal) subsets of $[0,L]$ as q increases.

Since D_1 is generally smaller than $D_0=1$, their difference

$$C_1 = 1-D_1 \geq 0 \tag{19}$$

can be viewed as a straightforward measure of intermittency (or sparseness) in the system, equality in (19) being attained for weakly variable fields. The exponent D_1 is known as the "information" dimension, making C_1 a codimension. For a log-normal cascade one has $C_1=\sigma^2/2\ln\lambda_0$, the numerical values chosen for Fig. 1 leading to $C_1\approx 0.1$. Although C_1 is possibly the most important exponent in this approach, another value of particular interest to us is D_2, the "correlation" dimension. It is directly related to the autocorrelation and energy spectrum exponents, at least for one-dimensional cascade models [32]: $\mu=1-\tau(2)$ hence $\beta=\tau(2)=D_2$, cf. Eqs. (2) and (3), and since we know that $D_2<D_1<D_0=1$, stationarity ($\beta<1$) is established.

B. Singularity properties of bounded cascade models

We now apply singularity analysis to the bounded model (9) and (10), letting $D_q^{(n)}$ denote the generalized dimensions of the nth level bounded cascade model. We show in Appendix B that

$$D_q^{(n)} = \frac{1}{q-1}\left\{q - \frac{1}{n}\sum_{i=1}^{n}\log_2[(1+f_i)^q+(1-f_i)^q]\right\}$$
$$n=1,2,\cdots\ (-\infty\leq q\leq\infty) . \tag{20a}$$

If $f_i\equiv\text{const}=1-2p$, i.e., letting $H=0$ in (12), we retrieve the standard log-binomial result [13]

$$D_q^{(n)} \equiv D_q = -\frac{1}{q-1}\log_2[p^q+(1-p)^q], \quad 0\leq p<\tfrac{1}{2} . \tag{20b}$$

For $q=2$ the correlation dimension D_2 coincides with the spectral exponent β quoted in Eq. (37b) for this singular one-dimensional model but, for the bounded case (11), the connection between β and D_2 fails due to the lack of (small scale) stationarity.

Taking the limits $q\to\pm\infty$ in (20a) we find

$$D_{\pm\infty}^{(n)} = 1-\frac{1}{n}\sum_{i=1}^{n}\log_2(1\pm f_i), \quad n=1,2,\ldots, \tag{21a}$$

which relate directly to the lower ($-\infty$) and upper ($+\infty$) bounds of the model. These exponents can be contrasted with the singular case (20b):

$$1<D_{-\infty}=-\log_2 p\leq\infty, \quad 0\leq p<\tfrac{1}{2}$$
$$0\leq D_{+\infty}=-\log_2(1-p)<1, \quad 0\leq p<\tfrac{1}{2} . \tag{21b}$$

Clearly we have $D_{\pm\infty}^{(\infty)}=1$ in (21a) as long as (9b) since then

$$\frac{1}{n}\sum_{i=1}^{n} f_i \to 0, \quad n\to\infty , \tag{22}$$

and this is sufficient to obtain

$$D_q^{(n)} \to D_q^{(\infty)} = D_q \equiv 1, \quad n\to\infty . \tag{23}$$

More precisely,

$$\lim_{M\to\infty}\frac{1}{M}\int_1^M 2^{-Ht}t^s dt < \infty, \quad 0<H\leq\infty, \quad s\geq 0 , \tag{24}$$

and this is sufficient to prove (22); the trade of convergence in (23) is determined by the convergence of the integral (24).

For $q=1$, we can apply the rule of l'Hospital to Eqs. (20a) and (20b) and obtain the following measures of intermittency $C_1^{(n)}$ at each cascade level n:

$$C_1^{(n)}=1-D_1^{(n)}=\frac{1}{2n}\sum_{i=1}^{n}[(1+f_i)\log_2(1+f_i)+(1-f_i)\log_2(1-f_i)],\quad f_i\to 0,\ i\to\infty \qquad (25a)$$

and

$$C_1^{(n)}\equiv C_1=1+p\log_2 p+(1-p)\log_2(1-p)\geq 0,\quad f_i\equiv 1-2p\ . \qquad (25b)$$

As mentioned earlier, the case $p=H=0$ corresponds to randomly positioned δ functions and $C_1=1$ in this (most intermittent) case. In the general bounded case (25a), we of course have

$$C_1^{(n)}\to C_1\equiv 0,\quad n\to\infty\ . \qquad (26)$$

Summarizing, the bounded ($H>0$) model is no longer a multifractal in the restricted sense of singular measures since these scale trivially in the limit of many cascade steps ($D_q\equiv 1, -\infty\leq q\leq\infty$), it is in the same class as homogeneous fields ($f_i\approx 0$) in spite of its intrinsically multiplicative character. In the singular limit $H=0$ the model becomes unbounded and, being identical to a microcanonical log-binomial model, has a nontrivial singularity spectrum. The most singular case, $H=p=0$, yields δ functions as a special type of fractal measure ($D_q=\infty$ for $q<0$, $D_q=1$ for $q=0$, and $D_q=0$ for $q>0$). However, we will soon see that the bounded model is multifractal in the broad sense since it has multiscaling structure functions (which, in fact, turn out to be trivial in the unbounded case). We will relate this radical change in statistical behavior to the transition from stationarity to nonstationarity. In the meantime, we will have a closer look at various parameter dependencies and reinterpret the lattice size effects we just evaluated in terms applicable to data analysis.

C. Boundedness and "residual" multifractality

For simplicity, we consider the two-parameter bounded cascade model described in Eqs. (10)–(12) and illustrated in Fig. 2. Figure 3(a) illustrates the dependence of generalized dimension $D_q^{(n)}$ on n, the number of cascade levels. As predicted in (23), $D_q^{(n)}$ tends to 1 with increasing n. If one fixes the number of cascade steps and varies the parameter H [Fig. 3(b)], the singularity of the bounded cascade model naturally increases as H decreases. The limit case $H=0$ represents a singular multifractal [the integral in (24) diverges] and differs considerably from finite H [e.g., 0.15 on Fig. 3(b)]. The closer p to 0.5 the smoother the field is and the smaller the difference between $D_q^{(n)}$ and 1 [Fig. 3(c)].

For truly intermittent multifractal process with $H=0$ the singularities are not smoothed with the increase of n. As a result, the generalized dimensions D_q of the singular model do not depend on n, at least in microcanonical situations such as ours. In essence, by "turning on" the smoothing parameter H we have gone from a stochastically discontinuous model to a stochastically continuous one. However, there always remains at finite resolution a

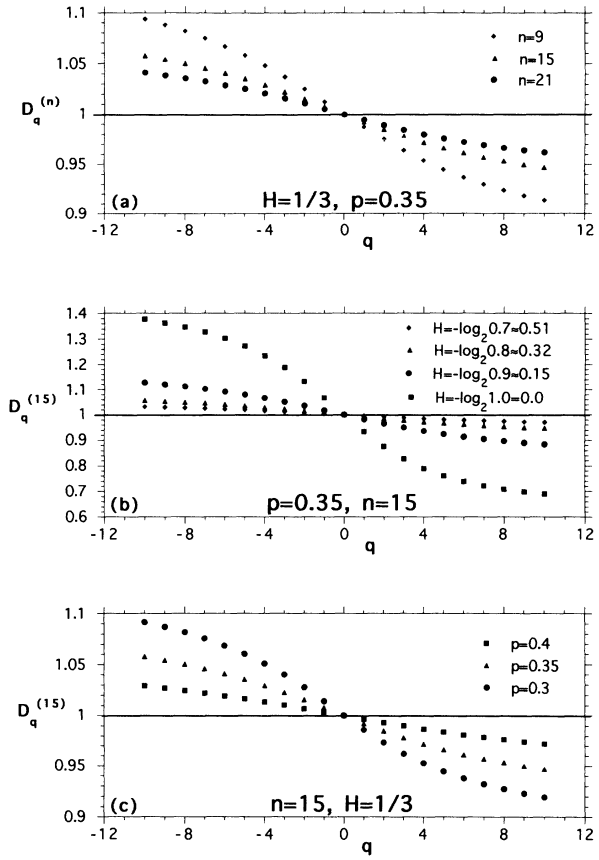

FIG. 3. Generalized dimensions D_q of the bounded cascade model: dependence on the parameters H, p, and n. (a) $H=\frac{1}{3}$, $p=0.35$, $n=9$, 15, and 21 (notice the convergence to unity); (b) $p=0.35$, $n=15$; $2^{-H}=0.7$, 0.8, 0.9 ("residual" multifractalities) and 1.0 (unbounded log-binomial truly multifractal model); (c) $H=\frac{1}{3}$, $n=15$; $p=0.30$, 0.35, 0.40 (increasing smoothness and accelerating the convergence to unity).

"residual" or "spurious" multifractality. In data-analysis applications, such residual multiscaling cannot be distinguished from *bona fide* multifractality associated with a sufficiently narrow singularity spectrum without improving the instrumental resolution (which is like increasing n).

IV. STRUCTURE FUNCTIONS

A. Brief description

Following as closely as possible the development in Sec. III A on singular measures, we return to (14) and slightly but importantly revise the definition of our generic stochastic process allowing $\varphi(x)$ to take *a priori* any real value. Instead of $I_{B_r}(x)$, we now take its antigradient (denoted $-\partial_x\equiv-\partial/\partial x$) as a scale-selective weighting function for the convolution operation in (15):

$$-\partial_x I_{B_r}(x)=\delta(x-r/2)-\delta(x+r/2),\quad 0<r\leq L\ .$$

This allows us to define the relative "increment" of $\varphi(x)$, over a distance r around x,

$$\Delta\varphi(r;x)=\varphi\circ\partial_x I_{B_r}(x)$$
$$=\varphi(x+r/2)-\varphi(x-r/2),$$
$$r/2\le x\le L-r/2\ . \quad (27)$$

In analogy with (16), we define the normalized random absolute increment

$$d_r(x)=\frac{|\Delta\varphi(r;x)|}{\langle|\Delta\varphi(L;L/2)|\rangle}\ge 0\ . \quad (28)$$

If the process $\varphi(x)$ has stationary increments, the statistical properties of $d_r(x)$ will not depend on x, e.g., $\langle d_r(x)^q\rangle=\langle d_r^q\rangle$ which are known as "structure functions."

For scaling processes, we readily anticipate

$$\langle d_r^q\rangle\sim\left(\frac{r}{L}\right)^{\zeta(q)},\quad 0<r\ll L \quad (29)$$

for q such that $\langle|\Delta\varphi(r)|^q\rangle<\infty$; this implies in particular, $q>-1$, unless vanishing increments are unusually rare (more on this limitation in Ref. [29]). In (29) L is viewed as the upper bound of the nonstationary scaling regime: r^* for the models described in (12) and (13), the integral scale more generally speaking. Like singular measures, structure functions are non-negative and conditioned by scale so many analogies can be drawn between the two approaches. There are, however, important differences as well. For instance, the normalized variables $d_r(x)$ are insensitive not only to multiplication of $\varphi(x)$ by a constant, as for the $p_r(x)$, but also to the addition of a constant. Exploiting this invariance and increment stationarity, one can substitute $\langle|\Delta\varphi(r)|^q\rangle=\langle|\Delta\varphi(r;x)|^q\rangle$ for $\langle d_r^q\rangle$ in (29) without loss of generality and will do so in the following. A wavelet-based family of analyzing functions that generalize $I_{B_r}(x)$ and $-\partial_x I_{B_r}(x)$ leading to further invariance properties is described in Ref. [29].

At the very least we know that, like $\tau(q)$, $\zeta(q)$ must be concave. One can also show that $\zeta(q)$ is nondecreasing, at least for bounded models based on cascade processes or not (details in Appendix A). As a counterpart to the exponent hierarchy D_q in (18), we will use

$$H_q=\frac{\zeta(q)}{q} \quad (30)$$

which is necessarily decreasing for any concave $\zeta(q)$, given that $\zeta(0)=0$ by definition. The scaling version of the Wiener-Khintchine relation applicable to processes with stationary increments [32] tells us that the spectral exponent is related to the case $q=2$,

$$\beta=2H_2+1\ge 1\ . \quad (31)$$

Another special case which has attracted much attention is $q=1$ since it can be related to the fractal dimension of the graph $g(\varphi)$ of $\varphi(x)$, viewed as an object in two-dimensional space [34]:

$$D_{g(\varphi)}=2-H_1\le 2 \quad (32)$$

where $H_1=\zeta(1)$ is the Hölder or "roughness" exponent in (29). This, incidentally, puts bounds on H_1, the codimension of $g(\varphi)$. The smallest possible $D_{g(\varphi)}$ is 1, attained for differentiable functions at $H_1=1$. Of course the upper bound on $D_{g(\varphi)}$ is 2 (the graph fills a two-dimensional space) and is attained for $H_1=0$, the corresponding ($q=1$) structure function is not only scale invariant but scale independent. This occurs for the stationary scaling processes, including all singular multifractal cascades. Finally, it is noteworthy that $H_1=\zeta(1)>0$ in (29) is equivalent to a statement of stochastic continuity, i.e., increments over small distances are (almost surely everywhere) small.

In Sec. III A, we had two predetermined exponents, $\tau(0)=-1$ and $\tau(1)=0$, and we retained $C_1=1-D_1=1-\tau'(1)$ in (19) as the single most important exponent in the whole approach based on singular measures. To first order, C_1 quantifies intermittency or sparseness viewed as a special kind of variability. Of course all the other exponents are necessary to qualify the intermittency hence the multifractality (in the sense of singular measures). For structure functions the situation is somewhat different. We have only one predetermined case, $\zeta(0)=0$, so if we can retain one single exponent from this approach, it will only account for the linear part of $\zeta(q)$. For simplicity, we will take the graph codimension $H_1=\zeta(1)$ in (32) not only as a direct measure of "smoothness" in the process but as a measure of the deviation from stationary behavior, a quantifier of nonstationarity in the observed variability [35]. All the other $\zeta(q)$ exponents will of course be necessary to qualify the nonstationarity or multiaffinity (multifractality in the sense of structure functions).

B. Self-affinity and multiaffinity

If the increments are narrowly distributed, then we will have $\langle|\Delta\varphi(r)|^q\rangle\approx\langle|\Delta\varphi(r)|\rangle^q$, and this immediately implies $\zeta(q)=q\zeta(1)=qH$, equivalently, $H_q\equiv H$, a constant not unrelated to the smoothing parameter in the bounded cascades (12), as we will soon see. For reasons given above in connection with $D_{g(\varphi)}$, we necessarily have $0<H<1$ and these models also have $\beta=2H+1$ for $q=2$. In this case, we are dealing with so-called self-affine processes which are characterized by simple (single exponent) but nontrivial statistical behavior from the viewpoint of structure functions. At any rate, this is the only case where one can justifiably say that

$$\langle|\Delta\varphi(\lambda r)|^q\rangle\approx\lambda^{qH}\langle|\Delta\varphi(r)|^q\rangle,\quad \lambda\ge 0\ . \quad (33)$$

The most standard definition of statistical self-affinity, a geometrical (graph-related) property, is retrieved at $q=1$ and need not be extended to $q\neq 1$ where there is no immediate geometrical interpretation of (33). We will refer to processes obeying (33) as monoscaling or, better still, "monoaffine" (see below).

The most famous self-affine random process is no doubt the standard Brownian motion (uncorrelated neighboring steps) the scaling of which is contained entirely the classical result $\langle|\Delta\varphi(r)|^2\rangle\sim r$ from which $\beta=2$ follows directly and $D_{g(\varphi)}=\frac{3}{2}$ from the associated $H=1/2$ monoscaling. For $H\neq 1/2$ (monoscaling) we obtain Mandelbrot's generalizations of Brownian motion

[23], known as fractional Brownian motions (FBM's). For $0<H<\frac{1}{2}$ $(1<\beta<2)$ we have negative correlations between neighboring steps, up to 50% anticorrelation in the stationary limit $H\to 0$, and for $\frac{1}{2}<H<1$ $(2<\beta<3)$ positive correlations, up to 100% correlation in the almost everywhere differentiable limit $H\to 1$.

It is clear that Eq. (33) is unnecessarily restrictive if taken as a definition of statistical self-affinity. In contrast with (33), one can combine Eqs. (27)–(30) into

$$\langle|\Delta\varphi(\lambda r)|^q\rangle \approx \lambda^{qH_q}\langle|\Delta\varphi(r)|^q\rangle, \quad \lambda\geq 0 . \tag{34}$$

Random functions with nonconstant H_q's [non-linear $\zeta(q)$'s] have been recently described as "multiaffine" [26,27]. This leaves the more general concept of multifractality to encompass multiscaling in both functions (H_q's) and measures (D_q's).

Indeed (29), or (34), is the basis of Parisi and Frisch's [3] original description of a multifractal, namely as functions having nontrivial combinations of many different local Hölderian-type singularities [i.e., values of $h(x)$ in $|\Delta\varphi(r;x)|\sim r^{h(x)}$], each living on a different sub-set $\{x\in[0,L], |\Delta\varphi(r;x)|\sim r^h\}$ with a different fractal dimension $D(h)$. By showing that $D(h)$ is the Legendre transform of $\zeta(q)+1$, the authors gave Eqs. (29) and (34) explicitly multifractal significance, however they did not describe any specific way of constructing such a multifractal. Stationary multifractals (i.e., standard multiplicative cascades) have been proposed in many different guises [10–13] but, to the extent of our knowledge, they had only monoscaling nonstationary counterparts (i.e., FBM's) until quite recently [11,25–29, 40]. As we will now show, bounded cascade models [24] constitute another class of nonstationary multiaffine stochastic processes.

C. Application to bounded models

Using real-space renormalization, we show in Appendix C that Eqs. (30) and (34) lead to

$$\zeta(q)=\begin{cases} qH, & 0\leq q\leq 1/H \\ 1, & 1/H\leq q\leq\infty \end{cases} \tag{35a}$$

for the bounded cascade models described in (12). A heuristic argument for large q goes as follows: boundedness implies the existence of a maximum increment $|\Delta\varphi|_{\max}$ on all scales and it will eventually dominate the higher-order moments; for sufficiently large q, our estimator of $\langle|\Delta\varphi(r)|^q\rangle$ is $|\Delta\varphi|^q_{\max}/\Lambda\propto r$ since $\Lambda=1/r$, hence $\zeta(q\gg 1)=1$.

We plotted in Fig. 4 the scaling exponents $\zeta(q)$ for different values of H, equal to 0, $\frac{1}{5}$, $\frac{1}{3}$, $\frac{1}{2}$, and 1. The exponents were calculated numerically using a modified Higuchi algorithm [36] and the numerical results closely follow their theoretical counterparts in (35a). The dotted lines in Fig. 4 illustrate the behavior of $\zeta(q)$ for H equal to $\frac{1}{3}$ (FBM), $\frac{1}{2}$ (standard Brownian motion) and 1 (the limit case of differentiable functions). The limit case $H=0$ is quite interesting; the numerics show a "residual" shift from $\zeta(q)\equiv 0$ in the sense of Sec. III C but for multiaffinity since it is traceable to the finite number of cascade steps used ($n=15$ here).

Equivalently to (35a), we have

$$H_q=\min\{H,1/q\}, \quad 0\leq q\leq\infty . \tag{35b}$$

Three remarkable moments—$q=1$, 2, and $1/H$—deserve more detailed consideration.

$q=1$. From (32) and (35b), we find

$$D_{g(\varphi)}=2-H_1=\max\{2-H,1\} . \tag{36}$$

For $H\geq 1$ bounded cascade models become statistically (and visually) indistinguishable from piecewise constant functions, i.e., "simple" curves with dimension 1. Figure 5 provides an example with $H=1.7$; only a few jumps generated by the first few cascade steps are visible. In the opposite limiting case of unbounded log-binomial cascade models ($H=0$), the resulting field is intermittent and stationary and its graph dimension is 2. In short, nonstationary bounded models are stochastically continuous ($H_1>0$), unbounded but stationary ones are not ($H_1=0$).

$q=2$. Second-order moments are associated with energy spectra. From (31) and (35b), we find

$$\beta=2H_2+1=\min\{2H,1\}+1, \quad H>0 , \tag{37a}$$

which is >1. The special case $H=\frac{1}{3}$ yields $\beta=\frac{5}{3}$, corresponding to Kolmogorov's [16] scaling law for fully developed turbulence. In its singular ($H=0$) incarnation, the model is stationary so (31) hence (37a) no longer apply; the spectral exponent β is then fully defined by p

$$\beta=D_2=-\log_2[1-2p(1-p)], \quad H=0 , \tag{37b}$$

which is <1. Both theoretical spectral exponents (37a) and (37b) are presented in Fig. 6. We notice that the

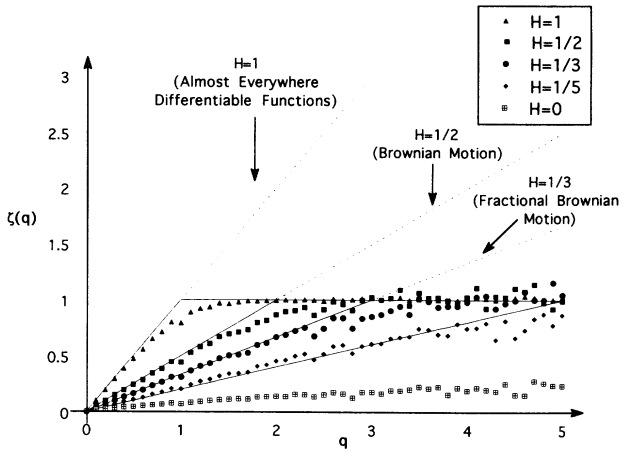

FIG. 4. Structure functions exponents $\zeta(q)$ of bounded and unbounded cascade models having $H=0$, $\frac{1}{5}$, $\frac{1}{3}$, $\frac{1}{2}$, and 1. Straight lines for FBM ($H=\frac{1}{3}$), standard Brownian motion ($H=\frac{1}{2}$), and differentiable functions ($H=1$) are added for comparison. The fluctuations in the data points are caused by the change of realization for every value of q and provide a useful indication of the deviation from ergodicity in our model. Notice also the systematic positive deviation of the unbounded $H=0$ case from $\zeta(q)\equiv 0$ as well as the "smoothing" of the transition at $q=1/H$; these are both effects of the finite resolution ($n=15$).

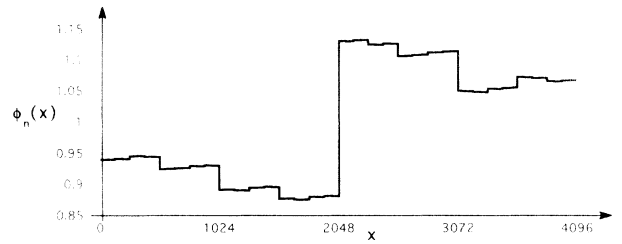

FIG. 5. Example of a bounded cascade model with extreme smoothness. The parameters are $H=1.7$, $p=0.35$ (for $n=12$) and lead to $H_1=1$, hence $D_g=1$ (almost everywhere differentiability); $H_2=1/2$, hence $\beta=2$ (a few discontinuities remain from the first cascade steps); and bounds $\phi_-=0.871\cdots$ and $\phi_+=1.13\cdots$.

singular limit of the bounded model ($H\to 0$) and the weak variability limit of the unbounded model ($p\to\frac{1}{2}$) agree ($\beta\to 1^{\pm}$) and, for all practical purposes, "flicker noise" ($\beta=1$) lies at the boundary between scaling processes that are stationary ($\beta<1$) and those that have stationary increments ($1<\beta<3$). [Going from (37b) to (37a) was in fact the original motivation for the bounded model [24].]

$q=q_c$. This is the moment of highest order where the $\zeta(q)$'s of bounded models with smoothing exponent H coincide with those of FBM's having an identical parameter; namely,

$$q_c=1/H\ .$$

Indeed, for $q>q_c$, we have $\zeta(1)=1$ for the bounded model (35a) and $\zeta(q)=qH$ for FBM in (33). In other words, bounded models and FBM's are indistinguishable by structure functions alone for all moments $q\le q_c$. It is noteworthy that for $H=\frac{1}{3}$ ($\beta=\frac{5}{3}$) the critical moment q_c equals 3. In the framework of multifractals and singularity analysis, the thermodynamical formalism [37] allows us to interpret a discontinuity in the derivative of any exponent function like $\zeta(q)$ as a (first-order) phase transition. In the present model, this qualitative change in statistical behavior for large q is traceable to the boundedness and related large scale stationarity, both of which are absent in FBM. This remarkable feature of the bounded model will be discussed in more detail elsewhere and contrasted with other interesting cases of multifractal phase transitions for structure functions [25,30,38].

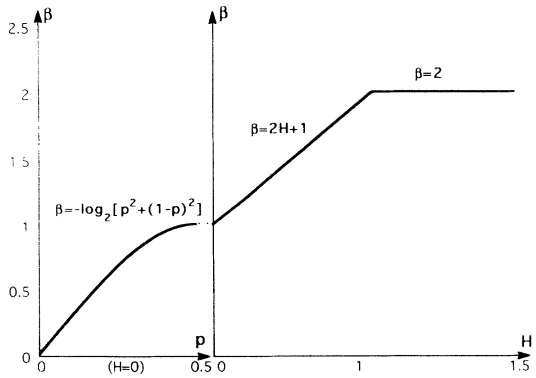

FIG. 6. Spectral exponents of bounded and unbounded cascade models. Notice the different parameters being varied horizontally. On the left-hand side ($0\le\beta\le 1$, stationarity prevails and $H=0$), p varies from 0 to $\frac{1}{2}$. On the right-hand side ($1\le\beta\le 2$, stationary increments prevail and p is irrelevant), H varies from 0 to 1.5; no change in p occurs beyond $H=1$.

V. DISCUSSION AND GEOPHYSICAL APPLICATIONS

We can visualize many of our findings with the help of Fig. 7 where we represent the position of our $\{p,H;n\}$-models in the "mean multifractal plane." In this representation the axes are both codimensions so we can directly compare arbitrary scalar fields $\varphi(x)$ with $x\in\mathbb{R}^D$ for any dimension D. Vertically, we use the information codimension $C_1=D-D_1=D-\tau'(1)$—a direct measure of intermittency—and horizontally, the graph codimension $H_1=(D+1)-D_g=\zeta(1)$—a direct measure of nonstationarity. In Refs. [15,35] we promote this simple device as a means to classify, compare, relate, etc., geophysical data and/or stochastic models. In this application, however, one should use the process itself to find H_1 and, due to nonstationarity, a related stationary measure (such as the absolute small-scale gradient field) is used to find C_1. Here we more simply use the bounded cascade to determine both coordinates, with one exception discussed in Table I.

All four corners of the natural domain $(H_1,C_1)\in[0,1]^2$ for $D=1$ are occupied by well-known cases, each of which can in turn be mapped to selected values of p and H (at $n=\infty$) for our model (cf. Table I). For finite n, we find the model to navigate very near the axes: vertically if $H=0$ (variable p), and horizontally if $H>0$ (any p). The distance from the axes decreases with increasing n so we are simply dealing with finite-size effects, "residual" intermittency or smoothness exponents (see inset in Fig. 7). Using the above described rules—C_1 relates to absolute gradients—we find the interior of the domain occupied by various geophysical datasets, such as cloud liquid water density [21], and other multiaffine models, such as fractionally integrated cascades [11,35].

It is of interest to note that both bounded [24] and fractionally integrated [11] cascades were largely motivated in the first place by cloud radiation problems. In the meteorological community, there is an urgent need for simple but realistic stochastic models for internal cloud structure. Cloud variability—the atmosphere's fluctuating liquid water and/or ice density field—is widely recognized as having a first-order effect in the Earth's radiation budget, hence on climate modulation. Uncertainties in cloud radiative properties are therefore one of the major sources of error in climate forecasting efforts. The bounded cascade model is applied directly to the cloud radiation problem in Ref. [39], using the parameter H only to fit the observed wave-number spectrum of the fluctuations of vertically integrated liquid water [$\beta=\zeta(2)+1\approx\frac{5}{3}$] and the parameter p is then used to approximate the observed one-point histogram, thus largely complementing this study.

Without eliminating the possibility of the existence of a natural signal with a complete $\zeta(q)$ spectrum that can be matched by that of the bounded model, it is too simple to

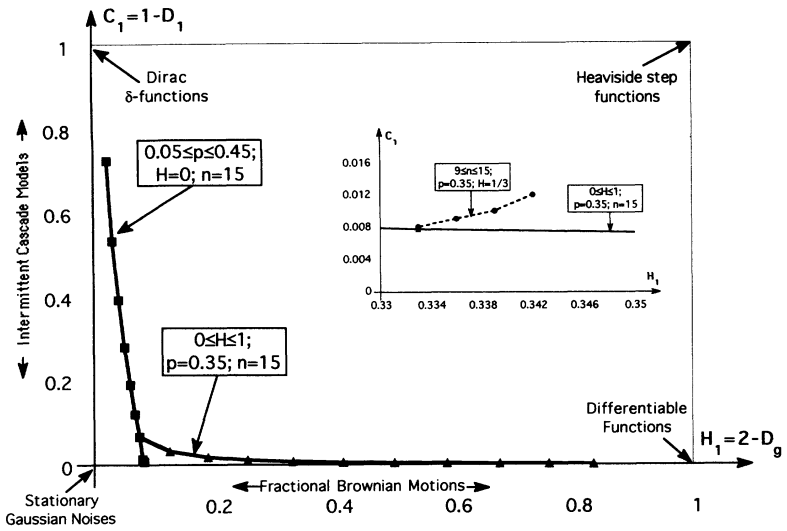

FIG. 7. Bounded and unbounded cascade models in the "multifractal $q=1$ plane." Vertically we have more and more intermittency, horizontally less and less stationarity. Note that the mapping of Heaviside step functions to the upper right hand corner assumes that the process itself is used for horizontal or H_1 positioning and its absolute gradient field (which is stationary) for vertical or C_1 positioning [15,35]. The inset illustrates "residual" intermittency: C_1 slowly converges to 0 with increasing resolution. See the text and Table I for further details.

be realistic and accordingly it has been exploited as a pedagogical tool, well suited for finding and exploring the boundary between stationarity and nonstationarity within the vast functional space defined by statistical scale invariance. It is hoped that, in turn, this knowledge can be of help in classifying natural phenomena and provide guidance for their statistical analysis.

VI. SUMMARY AND CONCLUSIONS

We have explored the statistical properties of cascade models (9) and (10) with multiplicative factors that approach unity as the cascade proceeds. In this case, the small-scale limit leads to fields that are bounded above and below. Special attention was given to model (12) which calls for an algebraic decay with respect to scale. Specifically the process $\phi(x)$ is defined on the interval [0,1] which is repeatedly divided in two, applying factors or "weights" $W=1\pm(1-2p)r_{n-1}^{H}$ $(0\le p\le\frac{1}{2},\ 0\le H\le\infty)$ at cascade step n where $r_n=2^{-n}$. Roughly speaking, the first few cascade steps—where the W's are still quite different from one—leave the field looking like a piecewise constant function, generally with rather large discontinuities; the following steps then modulate this field, basically in a weak additive manner. In essence, the large-scale features are multiplicative and stationary while their small-scale counterparts are additive and nonstationary (with stationary increments however).

Due to its boundedness, a standard singularity analysis of new model yields trivial results ($D_q\equiv 1$ for $n=\infty$). For finite n, however, nontrivial estimates of the D_q's are derived analytically [Eq. (20a), Fig. 3] and related to "residual" multifractality (i.e., one that is entirely traceable to finite-size effects). Nevertheless, the model has interesting multiscaling structure functions: $\zeta(q)$ in

$$\langle|\Delta\phi(r)|^q\rangle\sim\begin{cases} r^{\zeta(q)}\ , & r\ll 2^{-n^*}\ , \quad n^*=\dfrac{1}{H}\ , \quad q>-1 \\ \text{const}\ , & r\gtrsim 2^{-n^*}\ , \quad n^*=\dfrac{1}{H}\ , \quad q>-1\ , \end{cases}$$

is not linear in q. More precisely, we find [Appendix C, Eq. (35a), Fig. 4],

$$\zeta(q)\to\min\{qH,1\}\ ,\quad n\to\infty\ ,$$

whereas fractional Brownian motion (FBM) yields $\zeta(q)=qH$. In particular, the energy spectrum scales with an exponent $\beta=\zeta(2)+1>1$ whereas standard (unbounded) cascade models have $\beta<1$ (Fig. 6); however, this spectral exponent is not automatically related to the "roughness" exponent $H_1=\zeta(1)$ as in FBM's. The model is (asymptotically) multiaffine in a recently introduced nomenclature [26,27] where the FBM's are monoaffine and the concept of self-affinity only reflects on the fractal geometry of the graph at $q=1$, its dimension being $2-H_1$ [23,34].

The singular limit of the model ($H=0$) is equivalent to the p model [13] and then has trivial structure functions

TABLE I. Standard cases found in the four corners of the accessible "$q=1$" or "mean" multifractal domain, $(H_1,C_1)\in[0,1]^2$, for processes developing in $D=1$. Concerning Heaviside step functions, we use the function itself to obtain H_1 and its absolute gradient to obtain C_1; this is the recommended procedure when dealing with nonstationary geophysical data [15,35] and does not change the C_1 for the three first cases listed below.

C_1	H_1	Description	p	H
0	0	weakly variable scaling stationary noises	$\approx\frac{1}{2}$	0
0	1	nonconstant almost everywhere differentiable functions	$<\frac{1}{2}$	>1
1	0	Dirac δ functions	0	0
1	1	Heaviside step functions	$<\frac{1}{2}$	∞

$[\zeta(q)\equiv 0]$ due to the fully restored stationarity ($n^*=\infty$); numerically however ($n<\infty$), small $\zeta(q)$ values are found but they are residual. This shows that statistical analysis by singular measures on the one hand and by structure functions on the other largely complement rather than compete with each other. This is especially true when one leaves the realm of nonstationary stochastic models for that of nonstationary geophysical data analysis [15,21,35] where one must be particularly careful about finite-size effects.

In conclusion, we have analyzed a simple multiaffine stochastic model that is general enough to illustrate the key differences between scaling processes that are stationary and multiplicative, vs nonstationary and additive. Most importantly, the model allows the transition between these radically different stochastic "states" to be explored; in particular, the discontinuity in $\zeta'(q)$ at $q_c=1/H$ (a first-order multifractal phase transition) is directly related to the mixture of stationary and nonstationary ingredients in the present model. There is no doubt that such models will be helpful in understanding nonlinear phenomena in natural, computational and laboratory settings, a prime example (covering all three) being fully developed turbulence.

ACKNOWLEDGMENTS

This work was supported by U.S. Dept. of Energy's ARM (Atmospheric Radiation Measurement) program, Grant No. DE-A105-90ER61069 to NASA Goddard Space Flight Center. We thank A. Arnéodo, T. Bell, D. Lavallée, S. Lovejoy, C. Meneveau, and W. Ridgway for fruitful discussions.

APPENDIX A: A STATISTICAL CONSEQUENCE OF BOUNDEDNESS AND SCALE INVARIANCE

The concave function $\tau(q)$ has been well studied: it has been shown [8,11,33] that the r-conditioned moments $\langle p_r^q\rangle$ are divergent for all orders $q>q_D>q_m$, where the critical moment q_D is the solution of $\tau(q)=0$ (other than $q=1$) and q_m is the solution of $\tau'(q)=0$ (a maximum). So, if all moments are bounded ($q_D=\infty$), then concavity requires $\tau(q)$ to be a constant between $q_m\le\infty$ and ∞. For bounded models we can show that the same is true for $\zeta(q)$, namely that it is nondecreasing on $[0,\infty)$. More, generally, if

$$\langle|\Delta\varphi(r)|^q\rangle<\infty\ ,\quad r\to 0 \tag{A1}$$

then

$$\zeta'(q)\ge 0 \tag{A2}$$

where $\zeta(q)$ is defined in Eq. (29).

Indeed, let $q'>q$, then

$$\langle|\Delta\varphi(r)|^{q'}\rangle=\langle|\Delta\varphi(r)|^q|\Delta\varphi(r)|^{q'-q}\rangle \le \max_x|\Delta\varphi(r,x)|^{q'-q}\langle|\Delta\varphi(r)|^q\rangle\ .$$

It follows from this that

$$\max_x|\Delta\varphi(r,x)|^{q'-q}\ge\frac{\langle|\Delta\varphi(r)|^{q'}\rangle}{\langle|\Delta\varphi(r)|^q\rangle}\sim\frac{(r/L)^{\zeta(q')}}{(r/L)^{\zeta(q)}} =(r/L)^{\zeta(q')-\zeta(q)}\ . \tag{A3}$$

If one assumes that $\zeta(q')-\zeta(q)<0$ then

$$(r/L)^{\zeta(q')-\zeta(q)}\to\infty\ ,\quad r\to 0$$

since $r\ll L$ and, according to (A3), moment of order $q'-q>0$ is unbounded for small scales. This however contradicts (A1). Hence $\zeta(q')-\zeta(q)\ge 0$, i.e., the function $\zeta(q)$ is nondecreasing (A2).

Within the framework of incompressible turbulent flows, Frisch [41] explains the observed [42] nondecreasing $\zeta(q)$ for turbulent velocity structure functions using similar arguments; he furthermore justifies the bounds on velocity physically, invoking the speed of sound.

APPENDIX B: SINGULAR MEASURES OF BOUNDED CASCADE MODELS (9)

We derive here the generalized dimensions $D_q^{(n)}$ for all bounded cascade models (9).

First take $L=1$ and according to Eqs. (5)–(7) we have $\langle\Sigma\phi_n(1;\frac{1}{2})\rangle=\Sigma\phi_n(1;\frac{1}{2})=1/r_n=\Lambda_n=2^n$. Hence,

$$p_r(x_m)=\prod_{i=1}^{n}\frac{1\pm f_i}{2}\ ,\quad m=1,\ldots,\Lambda_n\ .$$

To simplify the below analysis we first show that

$$\ln\sum_{m=1}^{\Lambda_n}\left[\prod_{i=1}^{n}(1\pm f_i)\right]^q=\sum_{i=1}^{n}\ln[(1+f_i)^q+(1-f_i)^q]\ . \tag{B1}$$

Indeed, taking into account the microcanonical conservation of bounded model (9)–(10), the following chain of equalities proves Eq. (B1),

$$\begin{aligned}
\ln\sum_{m=1}^{\Lambda_n}\left[\prod_{i=1}^{n}(1\pm f_i)\right]^q &=\ln\left\{(1+f_1)^q\sum_{m=1}^{\Lambda_{n-1}}\left[\prod_{i=2}^{n}(1\pm f_i)\right]^q+(1-f_1)^q\sum_{m=1}^{\Lambda_{n-1}}\left[\prod_{i=2}^{n}(1\pm f_i)\right]^q\right\}\\
&=\ln\left[(1+f_1)^q+(1-f_1)^q\right]\left\{(1+f_2)^q\sum_{m=1}^{\Lambda_{n-2}}\left[\prod_{i=3}^{n}(1\pm f_i)\right]^q+(1-f_2)^q\sum_{m=1}^{\Lambda_{n-2}}\left[\prod_{i=3}^{n}(1\pm f_i)\right]^q\right\}\\
&=\cdots=\ln\{[(1+f_1)^q+(1-f_1)^q][(1+f_2)^q+(1-f_2)^q]\cdots[(1+f_n)^q+(1-f_n)^q]\}\\
&=\sum_{i=1}^{n}\ln[(1+f_i)^q+(1-f_i)^q]\ .
\end{aligned}$$

Then the sum of the qth power of p_r gives us

$$\langle p_r^q \rangle = r_n \sum_{m=1}^{\Lambda_n} \left[\prod_{i=1}^{n} \frac{1 \pm f_i}{2} \right]^q = r_n \exp \left[\ln \left\{ r_n^q \sum_{m=1}^{\Lambda_n} \left[\prod_{i=1}^{n} (1 \pm f_i) \right]^q \right\} \right]$$

$$= r_n^{q+1} \exp \sum_{i=1}^{n} \ln[(1+f_i)^q + (1-f_i)^q] = r_n^{q+1} \prod_{i=1}^{n} [(1+f_i)^q + (1-f_i)^q] ,$$

where $r_n = 2^{-n}$. Since (17b) and (18), one gets

$$(q-1) D_q^{(n)} = q - \frac{1}{n} \sum_{i=1}^{n} \log_2[(1+f_i)^q + (1-f_i)^q]$$

which is equivalent to Eq. (20a).

APPENDIX C: STRUCTURE FUNCTIONS OF BOUNDED CASCADE MODELS (12)

We present a real-space renormalization argument for our result in Eq. (35a). In the following, we use for convenience the original notations of Refs. [24,39]: $c = 2^{-H}$, $f_0 = (1-2p)2^H$.

1. First-order structure function

Theorem. If in the cascade model [Eqs. (9) and (10)] we take $f_i = f_0 c^i$, $f_0 > 0$, $0 < c \leq 1$, then the exponent $\zeta(1)$ defined as

$$\langle |\Delta\phi(\lambda r)| \rangle \sim \lambda^{\zeta(1)} \langle |\Delta\phi(r)| \rangle \tag{C1}$$

is

$$\zeta(1) = \begin{cases} -\log_2 c , & \frac{1}{2} \leq c \leq 1 \\ 1 , & 0 < c \leq \frac{1}{2} \end{cases} \tag{C2}$$

for all $\lambda = 2^j$, $j = 1, \ldots, n \gg 1$, where n is the number of cascade steps.

Proof. The absolute value of the smallest scale ($r = 1$) differences for the nth cascade level of a bounded model can be written as

$$\langle |\Delta\phi(r)| \rangle = \sum_{i=1}^{n} w_i^{(n)} \sum_{j=1}^{2^{i-1}} \langle \Delta_{ij} \rangle \tag{C3}$$

where the weights $w_i^{(n)}$ correspond to the probability of the absolute value of all possible differences. Since there are

$$\sum_{i=1}^{n} 2^{i-1} = 2^n - 1$$

weights, all together they should be normalized as

$$\sum_{i=1}^{n} \sum_{j=1}^{2^{i-1}} w_i^{(n)} = \sum_{i=1}^{n} 2^{i-1} w_i^{(n)} = 1 . \tag{C4}$$

One can prove by induction that

$$w_i^{(n)} = \frac{2^{n+1-2i}}{2^n - 1} \quad (i = 1, \ldots, n) \tag{C5}$$

which satisfies Eq. (C4).

The differences Δ_{ij} have common "parents,"

$$P_i = \prod_{l=1}^{n-i} 1 \pm f_l \quad (i = 1, \ldots, n)$$

and the index j ($j = 1, \ldots, 2^{i-1}$) denotes the number of all possible differences. Namely,

$$\Delta_{11} = 2P_1 f_n \ ; \ \Delta_{21} = 2P_2(1 \pm f_n) f_{n-1} \ ; \ \Delta_{22} = 2P_2(f_{n-1} \pm f_n) \ ;$$

$$\Delta_{31} = 2P_3 f_{n-2}(1 \pm f_{n-1})(1 \pm f_n); \ \Delta_{32} = 2P_3(f_{n-2} \pm f_n)(1 \pm f_{n-1}) \ ; \tag{C6}$$

$$\Delta_{33} = 2P_3(f_{n-2} \pm f_{n-1})(1 \pm f_n) \ ; \ \Delta_{34} = 2P_3(f_{n-2} \pm f_{n-1} \pm f_n \pm f_{n-2} f_{n-1} f_n) \ ; \text{ etc.}$$

We notice that there is a correlation between signs $\pm$ in (C6). However, it becomes negligible in the case of large

enough n and all derivations below are valid for $n \gg 1$ only.

After averaging (C6) and substituting $f_i = f_0 c^i$ into Eq. (C3) with $w_i^{(n)}$ defined by Eq. (C5), we get

$$\langle |\Delta\phi(r)| \rangle = \sum_{i=1}^{n} w_i^{(n)} [2 f_0 c^{n-i+1} 2^{i-1}] = f_0 \frac{(2c)^{n+1}}{2^n - 1} \sum_{i=1}^{n} (2c)^{-i} = f_0 \left| \frac{2c}{2^n - 1} \right| \frac{(2c)^n - 1}{2c - 1} \tag{C7}$$

for $c \neq 0.5$.

Let $\lambda = 2$ in Eq. (C1). It is not difficult to see that

$$\langle |\Delta\phi(2r)| \rangle = \sum_{i=2}^{n} 2 w_i^{(n-1)} \sum_{j=1}^{2^{i-1}} \langle \Delta_{ij} \rangle$$

and by analogy with (C7), one obtains

$$\langle |\Delta\phi(2r)| \rangle = f_0 \frac{2c}{2c - 1} \left| \frac{(2c)^{n-1} - 1}{2^{n-1} - 1} \right| , \quad c \neq \tfrac{1}{2} . \tag{C8}$$

Dividing (C7) by (C8) we get

$$\frac{\langle |\Delta\phi(r)| \rangle}{\langle |\Delta\phi(2r)| \rangle} = \frac{2^{n-1} - 1}{2^n - 1} \left| \frac{(2c)^n - 1}{(2c)^{n-1} - 1} \right| , \quad c \neq \tfrac{1}{2} . \tag{C9a}$$

Using the rule of l'Hospital we can easily find from Eq. (C9a) that

$$\frac{\langle |\Delta\phi(r)| \rangle}{\langle |\Delta\phi(2r)| \rangle} = \frac{2^{n-1} - 1}{2^n - 1} \left| \frac{n}{n - 1} \right| \tag{C9b}$$

for $c = 0.5$. Notice that Eq. (C9a) is not equal to 1 for $c = 1$ and all n because of the above-mentioned correlation. Moreover, one can prove that for $c = 1$ the ratio $\langle |\Delta\phi(r)| \rangle / \langle \Delta\phi(2r)| \rangle$ is always less than 1 and converges to 1 if $n \to \infty$.

It follows from Eqs. (C9a) and (C9b) that

$$\frac{\langle |\Delta\phi(r)| \rangle}{\langle |\Delta\phi(2r)| \rangle} \to \begin{cases} c , & 0.5 \leq c \leq 1 , \quad n \to \infty \\ \frac{1}{2} , & 0 < c \leq 0.5 , \quad n \to \infty . \end{cases} \tag{C10}$$

Taking (base 2) logarithms of both sides of (C10) yields Eq. (C2) for $\lambda = 2$. The theorem follows automatically for other values of $\lambda = 2^j$ ($j = 2, \ldots, n-1$) since

$$\langle |\Delta\phi(\lambda r)| \rangle = \langle |\Delta\phi(2^j r)| \rangle \sim 2^{\zeta(1)} \langle |\Delta\phi(2^{j-1} r)| \rangle \sim 2^{2\zeta(1)} \langle |\Delta\phi(2^{j-2} r)| \rangle \sim \cdots$$
$$\sim 2^{j\zeta(1)} \langle |\Delta\phi(r)| \rangle = \lambda^{\zeta(1)} \langle |\Delta\phi(r)| \rangle .$$

2. Structure functions for $q \neq 1$

In this subsection we generalize (nonrigorously) the theorem from the last section. Namely, to a first approximation (at least for $n \gg 1$), the exponents $\zeta(q)$ can be expressed as

$$\zeta(q) = \begin{cases} q(-\log_2 c) , & 0 \leq q \leq -1/\log_2 c \\ 1 , & -1/\log_2 c \leq q \leq \infty . \end{cases} \tag{C11}$$

Indeed,

$$\langle |\Delta\phi(r)|^q \rangle = \sum_{i=1}^{n} w_i^{(n)} \sum_{j=1}^{2^{i-1}} \langle \Delta_{ij}^q \rangle \approx f_0 \frac{(2c^q)^{n+1}}{2^n - 1} \sum_{i=1}^{n} (2c^q)^{-i} = f_0 \frac{2c^q}{2^n - 1} \left| \frac{(2c^q)^n - 1}{2c^q - 1} \right| ,$$

for $2c^q \neq 1$. The differences $\langle |\Delta\phi(2r)|^q \rangle$ are derived analogously. Then, one gets

$$\frac{\langle |\Delta\phi(r)|^q \rangle}{\langle |\Delta\phi(2r)|^q \rangle} \approx \frac{2^{n-1} - 1}{2^n - 1} \left| \frac{(2c^q)^n - 1}{(2c^q)^{n-1} - 1} \right| , \quad c \neq 2^{-1/q} \tag{C12}$$

which converges to c^q for $q \leq -1/\log_2 c$. If $q > -1/\log_2 c$ (i.e., $2c^q < 1$), the bracketed ratio in Eq. (C12) tends to 1 and (C12) itself converges to $\frac{1}{2}$, which immediately gives us (C11) and completes the renormalization-group argument for (35a) in the main body of the paper.

[1] P. Grassberger, Phys. Rev. Lett. **97**, 227 (1983).
[2] H. G. E. Hentschel and I. Procaccia, Physica D **8**, 435 (1983).
[3] G. Parisi and U. Frisch, in *Turbulence and Predictability in Geophysical Fluid Dynamics,* edited by M. Ghil, R. Benzi, and G. Parisi (Elsevier, Amsterdam, 1985), p. 84.
[4] C. T. Halsey, M. H. Jensen, L. P. Kadanoff, I. Procaccia, and B. I. Shraiman, Phys. Rev. A **33**, 1141 (1986).
[5] A. N. Kolmogorov, J. Fluid Mech. **13**, 82 (1962).
[6] A. Obukhov, J. Fluid Mech. **13**, 77 (1962).
[7] E. A. Novikov and R. Steward, Izv. Akad. Nauk SSSR, Ser. Geofiz. **3**, 408 (1964).
[8] B. B. Mandelbrot, J. Fluid Mech. **62**, 331 (1974).
[9] U. Frisch. P.-L. Sulem, and M. Nelkin, J. Fluid Mech. **87**, 719 (1978).
[10] D. Schertzer and S. Lovejoy, in *Turbulence and Chaotic Phenomena in Fluids,* edited by T. Tatsumi (Elsevier, New York, 1984), p. 505.
[11] D. Schertzer and S. Lovejoy, J. Geophys. Res. **92**, 9693 (1987).
[12] R. Benzi, G. Paladin, G. Parisi, and A. Vulpiani, J. Phys. A **17**, 3721 (1984).
[13] C. Meneveau and K. R. Sreenivasan, Phys. Rev. Lett. **59**, 1424 (1987).
[14] C. Meneveau, J. Fluid Mech. **232**, 469 (1991).
[15] A. Davis, A. Marshak, and W. Wiscombe, Fractals (to be published).
[16] A. N. Kolmogorov, Dokl. Akad. Nauk SSSR **30**, 299 (1941).
[17] A. Obukhov, Izv. Akad. Nauk. SSSR, Ser. Geogr. i Geofiz. **13**, 55 (1949).
[18] S. Corrsin, J. Appl. Phys. **22**, 469 (1951).
[19] W. D. King, C. T. Maher, and G. A. Hepburn, J. Appl. Meteor. **20**, 195 (1981).
[20] R. F. Cahalan and J. B. Snider, Remote Sens. Environ. **28**, 95 (1989).
[21] A. Marshak, A. Davis, W. Wiscombe, and R. Cahalan, J. Atmos. Sci. (to be published).
[22] S. Lovejoy *et al.*, Ann. Geophys. **11**, 119 (1993).
[23] B. B. Mandelbrot, *Fractals: Form, Chance, and Dimension* (W. H. Freeman, San Francisco, 1977).
[24] (a) R. F. Cahalan, M. Nestler, W. Ridgway, W. J. Wiscombe, and T. Bell, in *Proceedings of the 4th International Meeting on Statistical Climatology,* Roturua, New Zealand, edited by J. Sansom (New Zealand Meteorological Service, Wellington, NZ, 1990), pp. 28–32; (b) R. F. Cahalan and J. B. Snider, in the *Proceedings of the 9th Symposium on Turbulence and Diffusion,* Roskilde, Denmark (A.M.S., Boston, 1990), p. 11.
[25] A.-L. Barabási and T. Vicsek, Phys. Rev. A **44**, 2730 (1991).
[26] A.-L. Barabási, P. Szépfalusy, and T. Vicsek, Physica A **178**, 17 (1991).
[27] T. Vicsek and A.-L. Barabási, J. Phys. A: Math. Gen. **24**, L845 (1991).
[28] J. F. Muzy, E. Bacry, and A. Arnéodo, Phys. Rev. Lett. **67**, 3515 (1991).
[29] J. F. Muzy, E. Bacry, and A. Arnéodo, Phys. Rev. E **47**, 875 (1993).
[30] E. Bacry, J. F. Muzy, and A. Arnéodo, J. Stat. Phys. **70**, 635 (1993).
[31] A. Davis, A. Marshak, and W. Wiscombe (unpublished).
[32] A. S. Monin and A. M. Yaglom, *Statistical Fluid Mechanics,* Vol. 2 (MIT Press, Boston, 1975).
[33] D. Schertzer and S. Lovejoy, Physica A **185**, 187 (1992).
[34] K. J. Falconer, *The Geometry of Fractal Sets* (Cambridge University Press, Cambridge, 1986).
[35] A. Davis, A. Marshak, and W. Wiscombe, J. Geophys. Res. (to be published).
[36] T. Higuchi, Physica D **31**, 277 (1988).
[37] D. Katzen and I. Procaccia, Phys. Rev. Lett. **58**, 1169 (1987).
[38] A.-L. Barabási, R. Bourbonnais, M. Jensen, J. Kertész, T. Vicsek, and Y.-C. Zhang, Phys. Rev. A **45**, R6951 (1992).
[39] R. F. Cahalan, W. Ridgway, W. J. Wiscombe, T. Bell, and J. B. Snider, J. Atm. Sci. (to be published).
[40] R. Benzi, L. Biferale, A. Crisanti, G. Paladin, M. Vergassola, and A. Vulpiani, Physica D **65**, 352 (1993).
[41] U. Frisch, Proc. R. Soc. London, Ser. A **434**, 89 (1991).
[42] F. Anselmet, Y. Gagne, E. J. Hopfinger, and R. A. Antonia, J. Fluid Mech. **140**, 63 (1984).
[43] Throughout this paper we use φ to designate a generic random process and ϕ for our specific model. The latter type of symbol can be freely substituted into equations using the former.